HHS Public Access

Author manuscript

*J Mech Behav Biomed Mater*. Author manuscript; available in PMC 2019 August 01.

Published in final edited form as:

*J Mech Behav Biomed Mater*. 2018 August ; 84: 258–264. doi:10.1016/j.jmbbm.2018.05.019.

# The Rib Cage Stiffens the Thoracic Spine in a Cadaveric Model with Body Weight Load under Dynamic Moments

**Erin M. Mannen, Ph.D.**[a,1], **Elizabeth A. Friis, Ph.D.**[b,*], **Hadley L. Sis, M.S.**[c], **Benjamin M. Wong, M.S.**[d], **Eileen S. Cadel, M.S.**[e], and **Dennis E. Anderson, Ph.D.**[f]

[a]The University of Kansas, Department of Mechanical Engineering, Bioengineering Program, 1530 W. 15th St., Lawrence, KS 66045

[b]The University of Kansas, Department of Mechanical Engineering, Bioengineering Program, 1530 W. 15th St., Lawrence, KS 66045

[c]The University of Kansas, Bioengineering Program, 1530 W. 15th St., Lawrence, KS 66045

[d]The University of Kansas, Bioengineering Program, 1530 W. 15th St., Lawrence, KS 66045

[e]The University of Kansas, Bioengineering Program, 1530 W. 15th St., Lawrence, KS 66045

[f]Beth Israel Deaconess Medical Center, Center for Advanced Orthopaedic Studies, Harvard Medical School, Department of Orthopaedic Surgery, 330 Brookline Avenue, RN 115, Boston, MA 02215

## Abstract

The thoracic spine presents a challenge for biomechanical testing. With more segments than the lumbar and cervical regions and the integration with the rib cage, experimental approaches to evaluate the mechanical behavior of cadaveric thoracic spines have varied widely. Some researchers are now including the rib cage intact during testing, and some are incorporating follower load techniques in the thoracic spine. Both of these approaches aim to more closely model physiological conditions. To date, no studies have examined the impact of the rib cage on thoracic spine motion and stiffness in conjunction with follower loads. The purpose of this research was to quantify the mechanical effect of the rib cage on cadaveric thoracic spine motion and stiffness with a follower load under dynamic moments. It was hypothesized that the rib cage would increase stiffness and decrease motion of the thoracic spine with a follower load. Eight fresh-frozen human cadaveric thoracic spines with rib cages (T1–T12) were loaded with a 400 N compressive follower load. Dynamic moments of ±5 N·m were applied in lateral bending, flexion/extension, and axial rotation, and the motion and stiffness of the specimens with the rib cage intact

[*]Corresponding Author: EA Friis, The University of Kansas, Lawrence, KS USA, 1530 W 15th St., Learned Hall Room 3138, Lawrence, KS 66045, Phone: (785) 864-2104, Fax: (785) 864-5254.

[1]**Current Affiliation**: The University of Arkansas for Medical Sciences, Department of Orthopaedic Surgery 4301 W. Markham St. #531, Little Rock, AR 72205.

**CONFLICTS OF INTEREST**

The authors report no conflicts of interest.

have been previously reported. This study evaluated the motion and stiffness of the specimens after rib cage removal, and compared the data to the rib cage intact condition. Range-of-motion and stiffness were calculated for the upper, middle, and lower segments of the thoracic spine. Range-of-motion significantly increased with the removal of the rib cage in lateral bending, flexion/extension, and axial rotation by 63.5%, 63.0%, and 58.8%, respectively ($p<0.05$). Neutral and elastic zones increased in flexion/extension and axial rotation, and neutral zone stiffness decreased in axial rotation with rib cage removal. Overall, the removal of the rib cage increases the range-of-motion and decreases the stiffness of cadaveric thoracic spines under compressive follower loads *in vitro*. This study suggests that the rib cage should be included when testing a cadaveric thoracic spine with a follower load to optimize clinical relevance.

## 1. INTRODUCTION

One goal of cadaveric mechanical testing of the spine is to inform surgeons, device designers, and researchers of the potential mechanical impacts of implants or surgical techniques. While testing methods in both the cervical and lumbar spinal regions are well-defined, the thoracic region presents additional challenges due to the curvature, the 12-vertebrae length, and the presence of the rib cage preventing easy access to the spinal column. As medical device manufactures move to find motion preservation or growth-friendly solutions to scoliosis and other deformity issues that span the length of the spine, the thoracic region has become more important to study. Experimental setups are vastly different from lab to lab, so it is critical to recognize the limitations of cadaveric test methods so that results can be more fully understood. A few studies have shown that testing with an intact rib cage increases stiffness and decreases range-of-motion (ROM) and may more closely represent physiologic conditions when compared to models with no rib cage, thus researchers are beginning to include the rib cage during thoracic spine testing (Brasiliense et al., 2011; Healy et al., 2015, 2014; Liebsch et al., 2017; Lubelski et al., 2014; Mannen et al., 2015a; Watkins et al., 2005). However, previous cadaveric studies have not utilized loading conditions representative of body weight and active musculature on the cadaveric models, and published work from the current set of experiments has shown that compressive loading impacts disc pressures, motion, and stiffness in the thoracic spine (Anderson et al., 2016; Sis et al., 2016).

To mimic distribution of body weight and active musculature to increase the load carrying capacity of cadaveric models, researchers have developed a follower load methodology that is commonly used in the cervical and lumbar spine to distribute load through the vertebral column (Fry et al., 2014; Patwardhan et al., 2003, 2000, 1999). Follower loads may represent a more physiologically-accurate simulation of body weight and active musculature when compared to a pure compressive load across spinal segments of more than two levels. Follower-load methodology used in the cervical and lumbar spinal regions has been adapted for use in the thoracolumbar spine with no rib cage, but implementing a follower load in the thoracic spine presents additional challenges due to the presence of the rib cage (Stanley et al., 2004).

In published work from the same set of experiments reported in the current study, Sis et al. introduced a novel follower load technique allowing for the rib cage to remain intact and reported on the thoracic mechanics of 0 N, 200 N, and 400 N follower loads, highlighting the differences in ROM and stiffness when using a follower load with an intact rib cage (Sis et al., 2016). Anderson et al. then reported the static disc pressure and curvature changes resulting from various follower load levels and the dynamic disc pressure changes on thoracic cadaveric models, both with and without an intact rib cage (Dennis E Anderson et al., 2016; Anderson et al., 2017). However, no work has directly compared the mechanics of the thoracic spine with a follower load under dynamic loading with and without an intact rib cage. *The purpose of this study was to determine the mechanical contribution of the rib cage in the cadaveric thoracic spine during dynamic loading in lateral bending, flexion/extension, and axial rotation with a 400 N follower load representing body weight and active musculature.*

## 2. MATERIALS AND METHODS

### 2.1 Experimental Design

Eight fresh-frozen human cadaveric specimens (T1–T12) were dissected down to include only vertebrae, entire rib cage, intervertebral discs, and stabilizing ligaments. Although the removal of passive muscles may impact stiffness of the thorax, it was assumed that the application of the follower load accounted for active musculature and therefore the passive muscles could be removed. Specimens were screened to exclude severe osteophytes, vertebral fractures, spinal deformities, and previous thoracic spinal surgeries. Rib fractures were repaired with rigid stainless-steel plates and screws in one specimen using a technique that researchers claim does not influence the flexibility of the thorax (Watkins et al., 2005). Eight specimens were included in the study (four male, four female) with an average age of 66.9±4.4 years. Data on the impact of various follower load magnitudes and the changes in disc pressures have been previously reported on these specimens, though our prior manuscripts have not addressed the motion and stiffness impact of the rib cage on the thoracic spine with a follower load (Dennis E Anderson et al., 2016; Anderson et al., 2017; Sis et al., 2016).

Specimens were thawed to room temperature prior to testing. Figure 1A shows the experimental setup of a specimen with an intact rib cage. T1 and T12 were potted with Bondo auto-body filler (3M, St. Paul, MN, USA) with the inferior end mounted in a spine testing machine (Applied Test Systems, Butler, PA, USA) (Mannen et al., 2015). Motion-capture research pins with errors of 0.1 mm and 0.06° (Optotrak, Northern Digital Inc., Waterloo, ON, CAN) inserted into the potting at T1 and the left pedicles of T4 and T8 tracked the motion of the vertebrae. Additional motion capture pins at T2, T5, T9, and T11, and two pressure transducers in the intervertebral discs at T4–T5 and T8–T9 were used in other analyses not presented in this study.

A 400 N follower load was applied according to recently developed novel methods by Sis et al. and guided by studies from Patwardhan et al. (Patwardhan et al., 2003, 2000, 1999; Sis et al., 2016). Threaded steel rods were inserted into the center of the vertebral bodies of T3 through T11, and ball joint ends were screwed onto both sides. A steel cable was threaded

through holes in the potting at T1 and through each ball joint rod end, distributing the weight of the load through the vertebral bodies from T1 to T11. The inferior ends of the cables were threaded through pulleys positioned below to maintain spinal curvature. 200 N weights were hung at the ends of each of the cables, resulting in a 400 N follower load which is a reasonable magnitude to simulate the compressive loading experienced by the thoracic spine in upright standing (Dennis E Anderson et al., 2016). Figure 1B depicts the same follower load application once the rib cage has been removed. A six degree-of-freedom load cell fixed under the base of the specimen verified the resultant force acting on the spine was in the direction of the cables.

For each condition (rib cage intact and rib cage removed), a moment was applied to the unconstrained T1 potting at a displacement rate of 1 degree/second to a ±5 N·m load limit for five cycles in all three modes of bending (lateral bending, flexion-extension, and axial rotation). Specimens were manually loaded prior to each test to determine if the specimen could withstand the ±5 N·m moment without risk of irreversible damage based on observation. Saline solution was intermittently sprayed onto the specimens to maintain hydration. Analyses were conducted on the third cycle of data, and angular displacements of the upper (T1 to T4), middle (T4 to T8), and lower (T8 to T12) segments were calculated from the motion-capture pins (Wilke et al., 1998). The data from the rib cage intact condition has been reported previously as part of a set of parallel studies examining effect of follower-load magnitudes on motion and disc pressures, and all experiments from the set of studies on one specimen were conducted on the same day to avoid effects of multiple freeze-thaw cycles (Anderson et al., 2017; Sis et al., 2016).

### 2.2 Data and statistics

Data and statistical analyses were calculated using Matlab (MathWorks, Natick, MA, USA). Euler decompositions were used to calculate rotations (Crawford et al., 1996). Outcomes of interest were ROM, neutral zone (NZ), and elastic zone (EZ), and NZ and EZ stiffness, calculated for thoracic segmental motion for the upper, middle, and lower segments. Right- and left-lateral bending and right- and left-axial rotations have been found to be symmetric in the non-pathologic cadaveric spine, so mean parameters were found for right/left lateral bending, flexion, extension, and right/left axial rotation (Mannen et al., 2015b). Paired t-tests were conducted for each spinal region to determine the effect of the rib cage at $p<0.05$. It was hypothesized that ROM, NZ, and EZ will increase and NZ and EZ stiffness values will decrease with the removal of the rib cage.

## 3. RESULTS

Seven of the eight specimens were tested as planned. Mechanical integrity was a concern for one specimen in the rib cage removed condition during manual loading, so the specimen was loaded to only ±2 N·m; ROM, EZ, and EZ stiffness data were excluded for that specimen.

### 3.1 Range-of-motion

Angular displacement versus load data exhibited viscoelastic behavior, as shown in one cycle of a representative axial rotation trial for the middle thoracic section of both intact and

no rib cage conditions (Figure 2). The loading curves of the intact rib cage and no rib cage conditions are notably different both in ROM and stiffness. In nearly every case, the ROM in the no rib cage condition tends to increase when compared to the intact rib cage condition, with significant increases ranging from 18.3% to 95.6% in the different regions (Figure 3). Significant increases in overall ROM (the sum of the upper, middle, and lower motion segments) with no rib cage versus intact rib cage in lateral bending, flexion/extension, and axial rotation were 63.5%, 63.0%, and 58.8%, respectively ($p<0.05$) (Figure 4). Removal of the rib cage significantly increased the overall ROM compared with the intact rib cage in flexion and extension by 6.9° in each direction, totaling a 13.8° increase for the flexion/extension cycle (Figure 5).

The largest significant segmental increases in flexion/extension occurred in the middle thoracic segment in flexion (3.3°) and the lower thoracic segment in extension (4.4°). With the removal of the rib cage, significant increases in NZ were less than 0.7° for all segments, while significant increases in EZ varied from 1.0° to 3.3° (Figure 6). No significant differences in NZ or EZ were found in any segments in lateral bending. Table 1 shows the complete set of ROM, NZ, and EZ data.

### 3.2 Stiffness

Removal of the rib cage significantly decreased NZ stiffness by 82.7% in the upper region and 18.7% in the lower region during axial rotation ($p<0.05$), and trends toward decreasing stiffness by 40.2% in the middle region during flexion/extension ($p<0.1$). Trends of decreasing EZ stiffness by 31.3% and 46.1% were observed in the upper and middle regions during lateral bending, and by 53.2% in the lower region during axial rotation ($p<0.1$). However, no significant differences were seen in EZ stiffness. Table 2 shows the complete set of NZ and EZ stiffness data.

## 4. DISCUSSION

This study characterized the mechanical effect of the rib cage in dynamic tests of human cadaveric thoracic spines, with a follower load to simulate body weight and active musculature. The results show a notable increase in ROM and decrease in stiffness with the removal of the rib cage, a trend that was found in most motion segments for all modes of bending. This suggests that even with the added load-carrying capacity provided by a follower load, the rib cage continues to contribute significantly to the stability and stiffness of the thoracic spine. It has been shown that decreased stiffness in cadaveric specimens presents as instability in a clinical setting, so it is critical for researchers to understand the limitations of various cadaveric models (Pope and Panjabi, 1985).

Watkins et al. showed that the removal of the rib cage increases the flexibility of the human thoracic spine by up to 60%, though lower maximum moments were used compared to the present study (Watkins et al., 2005). Likewise, we previously found that testing a different set of cadaveric specimens without a rib cage increases ROM by 37%, 19%, and 77% and decreases NZ stiffness by 27%, 38%, and 58% in lateral bending, flexion/extension, and axial rotation, respectively (Mannen et al., 2015a). These results were supported by the recent work of Liebsch et al., which concluded that the rib cage impacts spinal rigidity in all

modes of bending, with an increase in axial rotation ROM by a factor of two (Liebsch et al., 2017). No follower load was applied in either of these previous studies; however, they represent the most similar experimental design to the present research. The present study shows similar ROM increases in axial rotation, and much larger increases in lateral bending and flexion/extension with the removal of the rib cage. This suggests that the rib cage remains a critical stabilizing structure in the thoracic spine in a cadaveric model with physiologically realistic levels of compressive loading.

The significant increase in EZ in the upper and middle regions during axial rotation with the removal of the rib cage calls into the question the mechanism for producing the characteristic elastic zone behavior. In the lumbar spinal region, EZ behavior is understood as the limits of motion primarily due to facet interaction (Kettler et al., 2008; Sharma et al., 1995). However, the results of the present study suggest that the rib cage also plays a significant role when examining the behavior at the limits of motion in the thoracic spine. The smaller and more obliquely-angled articulating facets in the thoracic region may not limit the axial rotation in the transverse plane in the same way as the larger, more perpendicularly-oriented lumbar facet joints. Thus, the importance of the rib cage in stabilizing the thoracic spine during axial rotation is critical. In addition to understanding the role of the rib cage, researchers should consider examining the roles of the costovertebral, costotransverse, and facet joints and major ligaments in the thoracic spine.

NZ stiffness values in the present study decrease significantly in lateral bending and flexion/extension with the removal of the rib cage when compared to similar testing done with no follower load (Mannen et al., 2015a). Many device manufacturers and surgeons are particularly interested in stiffness, because drastic changes in stiffness can lead to pain or instability (Pope and Panjabi, 1985). For these reasons, it is critical to understand the limitations of the cadaveric models used in the lab, both in ROM and stiffness, in order to best translate research findings to the operating room.

Brasiliense et al. studied the effect of the rib cage on upper-middle thoracic spinal motion in four-vertebrae segments (Brasiliense et al., 2011). Using an innovative technique to more evenly distribute the load to the most superior rib but without using a follower load, 7.5 N·m moments were applied in three modes of bending via a custom test machine. ROM increased with the removal of the rib cage by 182%, 181%, 702%, and 948% in lateral bending, flexion, extension, and axial rotation, respectively, compared to the middle thoracic segments in the current study which yielded increases of 140%, 112%, 103%, and 104%, respectively. These increases in ROM seem reasonable when compared to the present study, especially when considering that the loading technique of Brasiliense et al. resulted in <1° ROM values for flexion, extension and axial rotation in the intact condition. It is, however, difficult to compare these results directly due to the very different experimental setups.

Using a 400 N follower load in the thoracolumbar spine with no rib cage, Stanley et al. reported a 28° ROM in flexion/extension for T2-L1 (Stanley et al., 2004). This is comparable to the 34° ROM found for T1–T12 in the no rib cage condition in the present study, although load limits of 8 N·m and 6 N·m were used for flexion and extension, compared to 5 N·m in the present study.

Segmental motion was reported in lieu of overall motion for the present study. Due to the kyphotic upper and lordotic lower regions, the authors suggest that thoracic motion data may be best presented segmentally. Anderson et al. showed that with the application of various follower loads and rib cage conditions, while overall sagittal curvature was not significantly different, significant regional changes did occur (Dennis E Anderson et al., 2016). Figure 4 presents the summation of the segmental data in lieu of overall motion from the present study for the purpose of comparison to previous literature.

Thoracic cadaveric spine biomechanical research has inherent limitations. While the follower load techniques used in this study attempted to model physiologic body weight and active musculature, actual loading conditions in living humans are much more complicated. Stanley et al. has suggested an optimal follower load path be utilized in the thoracolumbar spine, however the techniques described were not reasonable to implement in this study on a spatially-constricted specimen with an intact rib cage (Stanley et al., 2004). Further, it is known that intra-abdominal pressure contributes significantly to the stability of the thorax, but researchers have not agreed on a way to appropriately mimic this in cadaveric models (Hodges et al., 2001). Follower loads are generally used only in flexion/extension in the cervical and lumbar regions, however the inclusion of a follower load in all modes of bending may be necessary in the thoracic region due to more complicated curvature, a longer vertebral column, and influence of intraabdominal pressure which is not generally accounted for in cadaveric models (D.E. Anderson et al., 2016; Sis et al., 2016). Without a follower load, particularly in a specimen with no rib cage, the cadaveric thoracic spine is extremely flexible in all planes and does not closely represent physiological loading conditions. It is in the field's best interest to further explore the development of follower load techniques for the thoracic spine in all modes of bending.

As with all cadaveric research, caution must be used when translating results to living patients. Because the goal of cadaveric research is to inform researchers and surgeons on the effects of devices or surgeries in living people, the link should be made between cadaveric research and human motion studies. Of particular importance, *in vivo* spine loading is not applied via pure moments, and *in vivo* thoracic spine ROM and stiffness would also depend on non-skeletal factors such as muscle strength, neuromuscular control, and pain during motions. *In vivo* human testing has the distinct advantage of obvious clinical relevance and translation to living people, however more variables exist when working with living human subjects, and in the case of this study, the rib cage could not be removed in living people. Understanding the unknown relationship between *in vitro* cadaveric thoracic studies and *in vivo* human motion will lead to a more accurate translation of cadaveric test results from the lab to the clinic. In addition, the ages of both human subjects and cadaveric specimens must always be considered, because thoracic flexibility decreases with age (Healy et al., 2014).

Likewise, computational models offer researchers the opportunity to study various experimental designs and to understand natural or pathological motion or the impact of surgical interventions on the thorax. Similar to cadaveric testing of the thorax, numerical simulation modeling of the thoracic spine and rib cage may be more complicated than cervical or lumbar regions due to the rib cage/spine interactions and intraabdominal pressure, and researchers are working to develop more physiologically-relevant

computational models by including the rib cage and/or intraabdominal pressure (Bruno et al., 2015; Meijer et al., 2011, 2010). Computational modeling remains a powerful tool in better understanding the impact of patient-specific anatomy, muscle interactions, disease, or surgery on motion and stiffness of the thorax, and the results of the present study can be used as validation metrics for computational models.

Overall, the hypotheses in this study were supported: the removal of the rib cage results in increased ROM and decreased stiffness in the human cadaveric spine with a follower load. The rib cage plays a significant mechanical role when testing a thoracic spine with a follower load, and future studies of thoracic spine mechanics should consider inclusion of the rib cage to enhance biomechanical validity and clinical relevance.

## Acknowledgments

The authors thank Dr. Sarah (Nikki) Galvis for help with testing.

**FUNDING**

This study was supported by the National Institutes of Health (NIH) National Institute on Aging (K99AG042458) and by a Mentored Career Development Award from the American Society for Bone and Mineral Research.

## References

Anderson, DE., Mannen, EM., Sis, HL., Wong, BM., Cadel, ES., Friis, EA., Bouxsein, ML. Effects of follower load and rib cage on intervertebral disc pressure and sagittal plane curvature in static tests of cadaveric thoracic spines; J Biomech. 2016. p. 49https://doi.org/10.1016/j.jbiomech.2016.02.038

Anderson, DE., Mannen, EM., Tromp, R., Wong, BM., Sis, HL., Cadel, ES., Friis, EA., Bouxsein, ML., Anderson, DE., Mannen, EM., Tromp, R., Wong, BM., Sis, HL., Cadel, ES., Friis, EA., Bouxsein, ML. The rib cage reduces intervertebral disc pressures in cadaveric thoracic spines by sharing loading under applied dynamic moments. J Biomech. 2017. https://doi.org/10.1016/j.jbiomech.2017.10.005

Brasiliense LB, Lazaro BC, Reyes PM, Dogan S, Theodore N, Crawford NR. Biomechanical contribution of the rib cage to thoracic stability. Spine (Phila Pa 1976). 2011; 36:E1686–93. https://doi.org/10.1097/BRS.0b013e318219ce84. [PubMed: 22138782]

Bruno AG, Bouxsein ML, Anderson DE. Development and Validation of a Musculoskeletal Model of the Fully Articulated Thoracolumbar Spine and Rib Cage. J Biomech Eng. 2015; 137:81003. https://doi.org/10.1115/1.4030408.

Crawford NR, Yamaguchi GT, Dickman CA. Methods for determining spinal flexion/extension, lateral bending, and axial rotation from marker coordinate data: Analysis and refinement. Hum Mov Sci. 1996; 15:55–78. https://doi.org/http://dx.doi.org/10.1016/0167-9457(95)00049-6.

Fry RW, Alamin TF, Voronov LI, Fielding LC, Ghanayem AJ, Parikh A, Carandang G, McIntosh BW, Havey RM, Patwardhan AG. Compressive preload reduces segmental flexion instability after progressive destabilization of the lumbar spine. Spine (Phila Pa 1976). 2014; 39:E74–81. https://doi.org/10.1097/brs.0000000000000093. [PubMed: 24153162]

Healy AT, Lubelski D, Mageswaran P, Bhowmick DA, Bartsch AJ, Benzel EC, Mroz TE. Biomechanical analysis of the upper thoracic spine after decompressive procedures. Spine J. 2014; 14:1010–1016. https://doi.org/10.1016/j.spinee.2013.11.035. [PubMed: 24291701]

Healy AT, Mageswaran P, Lubelski D, Rosenbaum BP, Matheus V, Benzel EC, Mroz TE. Thoracic range of motion, stability, and correlation to imaging-determined degeneration. J Neurosurg Spine. 2015; 23:170–177. https://doi.org/10.3171/2014.12.spine131112. [PubMed: 25978074]

Hodges PW, Cresswell AG, Daggfeldt K, Thorstensson A. In vivo measurement of the effect of intra-abdominal pressure on the human spine. J Biomech. 2001; 34:347–353. [PubMed: 11182126]

Kettler A, Drumm J, Heuer F, Haeussler K, Mack C, Claes L, Wilke H-J. Can a modified interspinous spacer prevent instability in axial rotation and lateral bending? A biomechanical in vitro study resulting in a new idea. Clin Biomech. 2008; 23:242–247. https://doi.org/10.1016/j.clinbiomech.2007.09.004.

Liebsch C, Graf N, Appelt K, Wilke HJ. The rib cage stabilizes the human thoracic spine: An in vitro study using stepwise reduction of rib cage structures. PLoS One. 2017; 12:e0178733. https://doi.org/10.1371/journal.pone.0178733. [PubMed: 28570671]

Lubelski, D., Healy, AT., Mageswaran, P., Benzel, EC., Mroz, TE. Biomechanics of the Lower Thoracic Spine Following Decompression and Fusion: A Cadaveric Analysis. Spine J. 2014. https://doi.org/10.1016/j.spinee.2014.03.026

Mannen EM, Anderson JT, Arnold PM, Friis EA. Mechanical Contribution of the Rib Cage in the Human Cadaveric Thoracic Spine. Spine (Phila Pa 1976). 2015a; 40:E760–6. https://doi.org/10.1097/brs.0000000000000879. [PubMed: 25768687]

Mannen EM, Anderson JT, Arnold PM, Friis EA. Mechanical analysis of the human cadaveric thoracic spine with intact rib cage. J Biomech. 2015b; 48:2060–2066. https://doi.org/10.1016/j.jbiomech.2015.03.021. [PubMed: 25912664]

Mannen EM, Ranu SS, Villanueva AM, Friis EA. Validation of a Novel Spine Test Machine. J Med Device. 2015; 9:11002. https://doi.org/10.1115/1.4028759.

Meijer GJM, Homminga J, Hekman EEG, Veldhuizen AG, Verkerke GJ. The effect of three-dimensional geometrical changes during adolescent growth on the biomechanics of a spinal motion segment. J Biomech. 43:1590–7. https://doi.org/10.1016/j.jbiomech.2010.01.028. [PubMed: 20206933]

Meijer GJM, Homminga J, Veldhuizen AG, Verkerke GJ. Influence of interpersonal geometrical variation on spinal motion segment stiffness. Spine (Phila Pa 1976). 2011; 36:929–935. https://doi.org/10.1097/BRS.0b013e3181fd7f7f.

Patwardhan AG, Havey RM, Carandang G, Simonds J, Voronov LI, Ghanayem AJ, Meade KP, Gavin TM, Paxinos O. Effect of compressive follower preload on the flexion-extension response of the human lumbar spine. J Orthop Res. 2003; 21:540–546. https://doi.org/10.1016/s0736-0266(02)00202-4. [PubMed: 12706029]

Patwardhan AG, Havey RM, Ghanayem AJ, Diener H, Meade KP, Dunlap B, Hodges SD. Load-carrying capacity of the human cervical spine in compression is increased under a follower load. Spine (Phila Pa 1976). 2000; 25:1548–1554. [PubMed: 10851105]

Patwardhan AG, Havey RM, Meade KP, Lee B, Dunlap B. A follower load increases the load-carrying capacity of the lumbar spine in compression. Spine (Phila Pa 1976). 1999; 24:1003–1009. [PubMed: 10332793]

Pope MH, Panjabi M. Biomechanical definitions of spinal instability. Spine (Phila Pa 1976). 1985; 10:255–256. [PubMed: 3992345]

Sharma M, Langrana NA, Rodriguez J. Role of ligaments and facets in lumbar spinal stability. Spine (Phila Pa 1976). 1995; 20:887–900. [PubMed: 7644953]

Sis HL, Mannen EM, Wong BM, Cadel ES, Bouxsein ML, Anderson DE, Friis EA. Effect of follower load on motion and stiffness of the human thoracic spine with intact rib cage. J Biomech. 2016; 49:3252–3259. https://doi.org/10.1016/j.jbiomech.2016.08.003. [PubMed: 27545081]

Stanley SK, Ghanayem AJ, Voronov LI, Havey RM, Paxinos O, Carandang G, Zindrick MR, Patwardhan AG. Flexion-extension response of the thoracolumbar spine under compressive follower preload. Spine (Phila Pa 1976). 2004; 29:E510–4. [PubMed: 15543052]

Watkins R 4th, Watkins R 3rd, Williams L, Ahlbrand S, Garcia R, Karamanian A, Sharp L, Vo C, Hedman T. Stability provided by the sternum and rib cage in the thoracic spine. Spine (Phila Pa 1976). 2005; 30:1283–1286. [PubMed: 15928553]

Wilke HJ, Wenger K, Claes L. Testing criteria for spinal implants: recommendations for the standardization of in vitro stability testing of spinal implants. Eur Spine J. 1998; 7:148–154. [PubMed: 9629939]

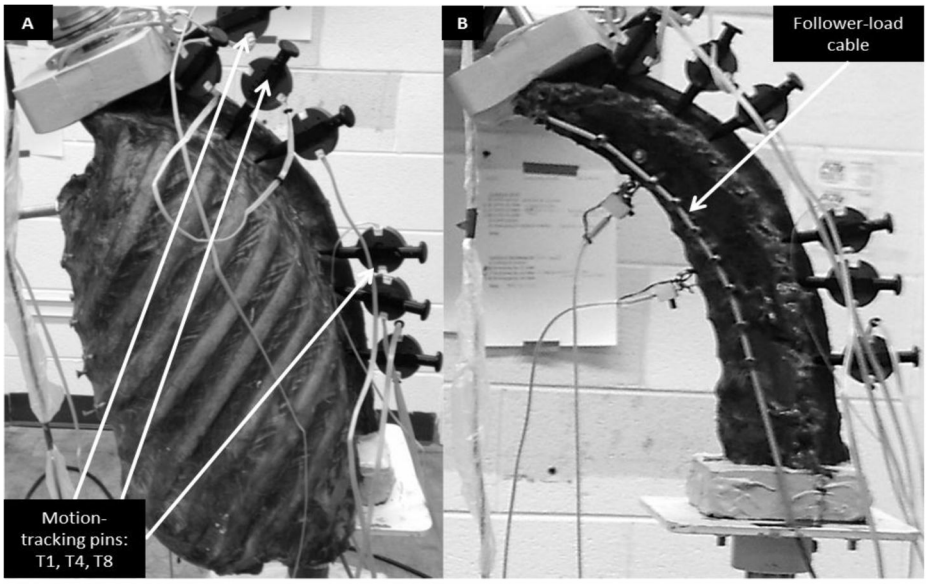


**Figure 1.**

Experimental setup with (A) intact rib cage and (B) no rib cage, both with a 400 N follower load. Motion tracking markers used in this study were placed at T1, T4, and T8 as indicated, and a follower load cable is noted.

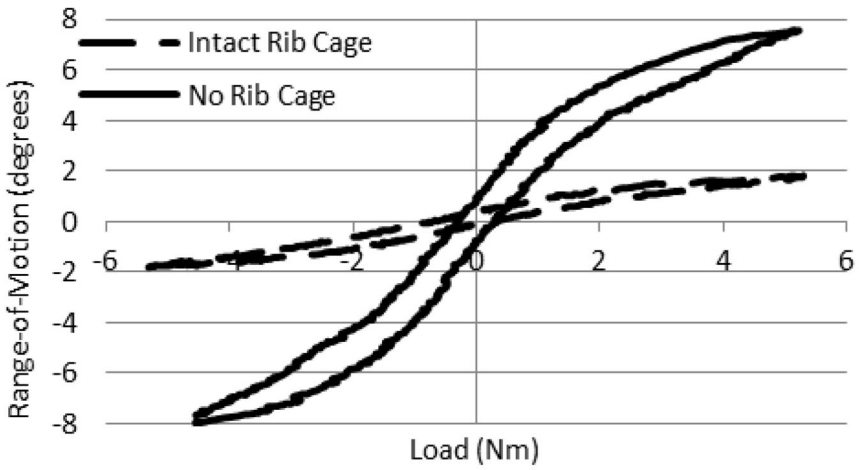


**Figure 2.**

Typical axial rotation range-of-motion versus moment curves for one cycle of a middle thoracic region with a 400 N follower load. The dotted line represents the intact rib cage condition, and the solid line represents the no rib cage condition.

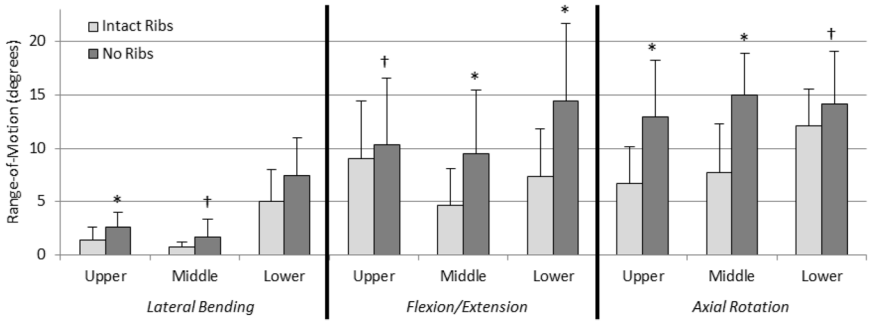


**Figure 3.**

Mean ± standard deviation of range-of-motion values for all thoracic spinal regions (upper, middle, and lower) for all modes of bending (lateral bending, flexion/extension, and axial rotation) for the intact rib cage and no rib cage conditions of human thoracic spines with 400 N follower loads under ±5 N·m dynamic moments (*$p<0.05$ †$p<0.1$).

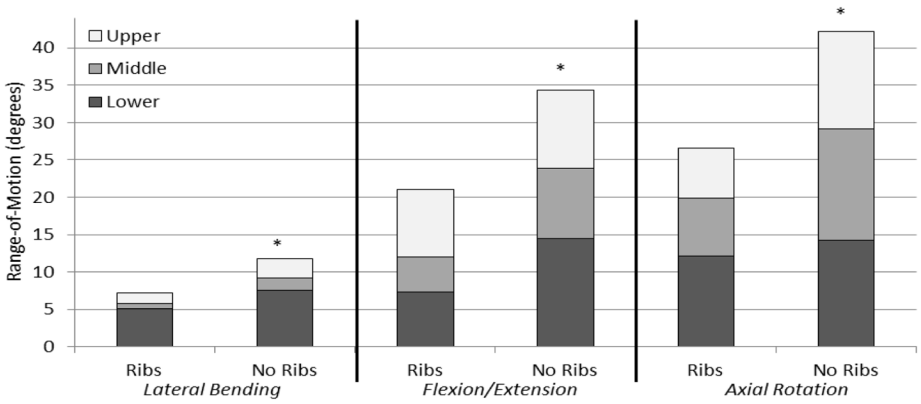


**Figure 4.**

Combined segmental range-of-motion data (T1 to T12) in all modes of bending (lateral bending, flexion/extension, and axial rotation) for the intact rib cage and no rib cage conditions for human thoracic spines with 400 N follower loads under ±5 N·m dynamic moments (*$p<0.05$).

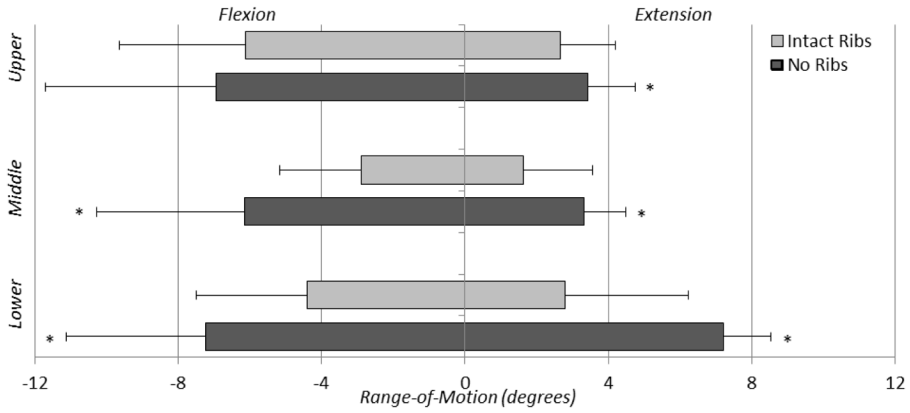


**Figure 5.**

Mean ± standard deviation of range-of-motion showing asymmetry in flexion versus extension for both the intact rib cage and no rib cage conditions for human thoracic spines with 400 N follower loads under ±5 N·m dynamic moments (*$p<0.05$).

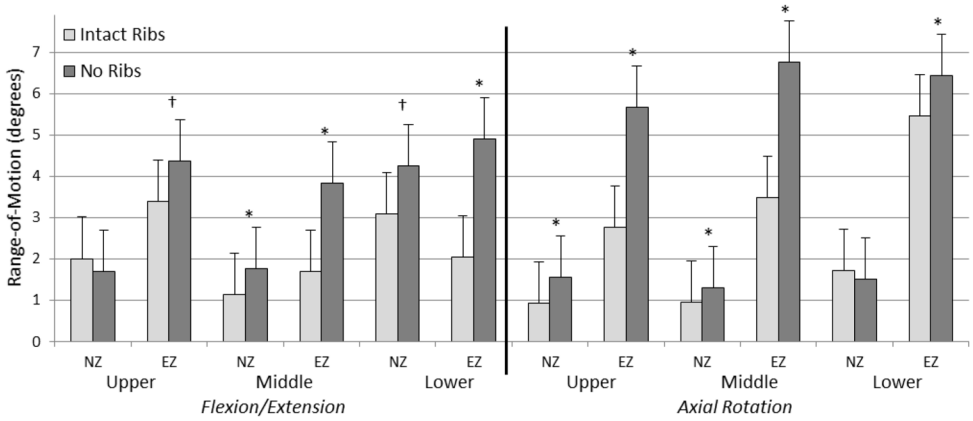


**Figure 6.**

Mean ± standard deviation of neutral and elastic zone range-of-motions for all regions (upper, middle, and lower) in flexion/extension and axial rotation, for both the intact rib cage and no rib cage conditions of human thoracic spines with 400 N follower loads under ±5 N·m dynamic moments (*$p<0.05$; †$p<0.1$).

*J Mech Behav Biomed Mater*. Author manuscript; available in PMC 2019 August 01.

**Table 1**

Means (standard deviations) of range-of-motion (ROM), neutral zone (NZ), and elastic zone (EZ) of upper (T1/T4), middle (T4/T8), and lower (T8/T12) thoracic segments for all modes of bending for intact rib cage and no rib cage conditions of human thoracic spines with 400 N follower loads under ±5 N·m dynamic moments (*p<0.05, †p<0.1).

| | | Lateral Bending | | | Flexion/Extension | | | Axial Rotation | | | Flexion | Extension |
|---|---|---|---|---|---|---|---|---|---|---|---|---|
| **Segment** | **Condition** | **ROM(°)** | **NZ(°)** | **EZ(°)** | **ROM(°)** | **NZ(°)** | **EZ(°)** | **ROM(°)** | **NZ(°)** | **EZ(°)** | **ROM(°)** | **ROM(°)** |
| Upper (T1/T4) | Intact Ribs | 1.43 (1.21) | 0.34 (0.23) | 0.57 (0.49) | 9.07 (5.35) | 2.01 (1.49) | 3.40 (1.75) | 6.69 (3.42) | 0.94 (0.69) | 2.76 (1.60) | 6.13 (3.52) | 2.67 (1.32) |
| | No Ribs | 2.58* (1.39) | 0.44 (0.38) | 1.07† (0.62) | 10.37† (6.25) | 1.71 (0.76) | 4.38† (2.80) | 12.98* (5.46) | 1.56* (0.72) | 5.66* (2.50) | 6.95 (4.76) | 3.42* (1.54) |
| Middle (T4/T8) | Intact Ribs | 0.71 (0.53) | 0.59 (0.21) | 0.22 (0.13) | 4.64 (3.50) | 1.13 (1.18) | 1.70 (1.20) | 7.72 (5.05) | 0.95 (1.03) | 3.48 (1.98) | 2.90 (2.28) | 1.63 (1.17) |
| | No Ribs | 1.71† (1.64) | 0.83 (0.69) | 0.44 (0.60) | 9.47* (6.01) | 1.78* (0.75) | 3.83* (2.67) | 14.99* (3.26) | 1.30* (0.63) | 6.76* (1.63) | 6.15* (4.15) | 3.32* (1.93) |
| Lower (T8/T12) | Intact Ribs | 5.14 (2.95) | 3.84 (2.27) | 0.65 (0.42) | 7.33 (4.49) | 3.09 (2.34) | 2.05 (1.07) | 12.16 (3.79) | 1.73 (1.38) | 5.45 (1.48) | 4.40 (3.12) | 2.79 (1.32) |
| | No Ribs | 7.50 (3.27) | 5.56 (2.87) | 0.97 (0.29) | 14.46* (7.29) | 4.26† (3.58) | 4.90* (1.96) | 14.22† (4.53) | 1.51 (0.68) | 6.44* (2.18) | 7.24* (3.89) | 7.22* (3.45) |

*J Mech Behav Biomed Mater*. Author manuscript; available in PMC 2019 August 01.

**Table 2**

Means (standard deviations) of neutral zone stiffness (NZS) and elastic zone stiffness (EZS) of upper (T1/T4), middle (T4/T8), and lower (T8/T12) thoracic segments for all modes of bending for intact rib cage and no rib cage conditions of human thoracic spines with 400 N follower loads under ±5 N·m dynamic moments (*p<0.05; †p<0.1)

| | | Lateral Bending | | Flexion/Extension | | Axial Rotation | |
|---|---|---|---|---|---|---|---|
| **Segment** | **Condition** | **NZS** | **EZS** | **NZS** | **EZS** | **NZS** | **EZS** |
| Upper (T1/T4) | Intact Ribs | 5.66 (3.84) | 6.85 (2.09) | 1.05 (0.62) | 2.29 (1.75) | 2.94 (4.42) | 3.28 (3.60) |
| | No Ribs | 3.12 (3.04) | 4.70† (1.58) | 1.29 (1.09) | 2.12 (1.31) | 0.51* (0.31) | 1.35 (0.59) |
| Middle (T4/T8) | Intact Ribs | 8.87 (4.46) | 8.30 (5.50) | 3.27 (3.91) | 4.74 (4.10) | 2.04 (2.49) | 4.51 (6.13) |
| | No Ribs | 5.45 (3.63) | 4.48† (3.53) | 1.95† (2.25) | 3.36 (2.17) | 0.42 (0.14) | 1.08 (0.27) |
| Lower (T8/T12) | Intact Ribs | 3.10 (1.25) | 2.87 (4.72) | 1.79 (1.72) | 2.97 (2.23) | 0.59 (0.29) | 2.31 (2.89) |
| | No Ribs | 2.68 (2.38) | 1.50 (0.80) | 0.89 (0.35) | 1.39† (0.35) | 0.48* (0.29) | 1.02 (0.33) |